Journal of Computer-Aided Molecular Design, **16:** 585–600, 2002.
KLUWER/ESCOM

Metal complexes of chiral pentaazacrowns as conformational templates for β-turn recognition

Andrea J. H. Reaka[1], Chris M. W. Ho[1] & Garland R. Marshall[1,2,*]
[1]*Center for Computational Biology, Washington University, St. Louis, MO 63110, U.S.A, and* [2]*MetaPhore Pharmaceuticals, Inc. 1910 Innerbelt Business Center Drive, St. Louis, MO 63114, U.S.A.*

Received 30 November 2001; Accepted 10 October 2002

Key words: β-turn mimetics, conformational templates, drug design, FOUNDATION, pentaazacrowns, receptor probes, metal complexes

Summary

Examples of reverse turns as recognition motifs in biological systems can be found in high-resolution crystal structures of antibody-peptide complexes. Development of peptidomimetics is often based on replacing the amide backbone of peptides by sugar rings, steroids, benzodiazepines, or other hetero- and carbocycles. In this approach, the chemical scaffold of the peptide backbone can be replaced while retaining activity as long as the pharmacophoric groups of the peptide side chains stay in relatively the same place; in other words, similar functional groups must overlap in space for interaction with critical receptor sites. This study evaluates the potential of metal complexes of chiral pentaazacrowns (PAC) derived by reduction of cyclic pentapeptides as β-turn mimetics. Due to the limited flexibility of the pendant chiral side groups in these metal complexes, one can potentially elicit information about the receptor-bound conformation from their binding affinities. 11 PAC crystal structures with different substitution patterns complexed with 3 different metals (Mn, Fe, Cd) as a prototypical database of potential side-chain orientations. Complexation with different metals induces subtle differences in the conformations of a particular azacrown scaffold. The lack of parameterization of transition metals for force field calculations precludes a thorough theoretical study. Thus, this study utilizes a simple geometrical comparison between the experimental data for crystalline PAC complexes and the side-chain orientations seen in classic β-turns. The FOUNDATION program was used to overlap the C_α-C_β vectors of the corresponding ideal β-turn side-chains to all possible leaving groups of the PAC complexes. When comparing the relative orientations of the chiral side chains, a strong overlap of the bonds (between about 0.1 Å to about 0.5 Å RMS for 3 residues and up to about 1 Å RMS for 4 residues) was observed for many of the molecules. Such metal complexes may lack complete peptidomimetic activity due to the lack of spatial overlap of all four side-chain residues, however, if only three peptide side chains are needed for receptor recognition and/or binding, the metal complexes should show biological activity.

Introduction

As high-throughput biological screening has gained popularity, peptide and peptidomimetic libraries have been instrumental in producing hundreds of thousands of different compounds for this process. At the same time, cloning and expressing of potential therapeutic targets has become routine to provide reagents for screening and possible structural determination, a prerequisite for structure-based drug design. The main obstacle for rational drug design for many biological systems, however, is the lack of information about the three-dimensional structure of the peptide in the receptor-ligand complex. This is often due to the limited information regarding the three-dimensional structure of the receptor, or other therapeutic target, despite the rapid progress in structural determination by crystallography and NMR spectroscopy. Studies of the isolated ligand or therapeutic target alone can be misleading since the bound structure of the ligand-

*Correspondence.

receptor complex is often different from the combined structures of the unbound ligand and receptor [1, 2]. Current indirect methods attempt to deduce the structure by interpreting the response of the receptor based on consistent data from biological testing. Then, by iterative chemical modification and subsequent biological testing, a hypothesis of the receptor-bound conformation may be generated [3]. Conformationally restricted peptides are the subject of increasing interest as potential new bioactive molecules. Peptide mimics with amide bonds and amino acid side chains dispersed in a more rigid arrangement can give valuable information on the bioactive conformation of the mimicked peptide in the complex with its receptor. Moreover, peptidomimetics with potential therapeutic value may result that display beneficial features such as enhanced oral bioavailability and metabolic stability.

Reverse turns are common secondary structural features and recognition sites in proteins [4]. Receptor recognition, substrate specificity, and catalytic function generally reside in these loop regions that often connect residues of the α helices and β strands contributing to the structural stability of proteins. β-turns, the most common type of reverse turn comprised of four residues, are characterized by their Φ_2, Ψ_2, Φ_3, and Ψ_3 torsion angles. The classic β-turn is stabilized by an intramolecular hydrogen bond between the carbonyl oxygen of residue i to the amide hydrogen of residue $i + 3$, although this is not an essential feature of four-residue reverse turns common in proteins. The distance between these heteroatoms for a reasonable hydrogen bond is 2.8–3.0 Å. β-turns are often conserved during evolution, and have been shown to be involved in molecular recognition [1, 4, 5] and considered as initiation sites for protein folding [6]. Development of compounds designed to mimic these secondary-structural features of β-turns has been an important aspect of elucidating the receptor-bound conformation of a biologically active peptide. Conformationally restricted β-turn mimics, with the amino acid side chains in a relatively rigid arrangement, can give valuable information about the bound conformation of the mimicked peptide [7, 8] when incorporated into the native sequence, if they retain activity. Thus, β-turn mimetics provide a conformational template for probing the receptor for its spatial requirements for molecular recognition.

Examples of turns as recognition motifs can be found in the literature in high-resolution crystal structures of antibody-peptide complexes [5, 9, 10]. Current activity in the development of peptidomimetics is based on replacing the amide backbone of peptides by sugar rings, steroids, benzodiazepines, or other hetero- and carbocycles. In this approach, the chemical scaffold of the peptide backbone can be replaced while retaining activity as long as the pharmacophoric groups of the peptide side chains stay in relatively the same place; in other words, similar functional groups must overlap in space for interaction with critical receptor sites. X-ray structures of peptides complexed with antibodies [5, 9, 10] are consistent with receptor recognition of turn motifs determined by structure-activity studies of the peptide hormones angiotensin II [11, 12], bradykinin [13, 14], GnRH (gonadotrophin-releasing hormone, LHRH) [15, 16], somatostatin [17, 18], and many others.

Cyclic and bicyclic dipeptide analogs have been developed to stabilize the reverse-turn in a peptide chain [19–23]. The dipeptide lactam [24], the bicyclic dipeptide BTD [25], and similar proline derivatives [26], spirolactam-bicyclic and tricyclic systems based on proline [27–30], substitution by α,α-dialkylamino acids [31–33], N-aminoproline [34], functionalized dibenzofurans [35–37], and substitution by dehydroamino acids [38–41] are all examples which enhance reverse-turn propensity [42, 43]. Other turn mimetics have focused on stabilizing a type VI β-turn with a cis-amide bond between residues $i + 1$ and $i + 2$ through disulfide bonds [18, 44]. This can also be accomplished by incorporation of tetrazole rings as cis-amide bond surrogates [45–47], incorporation of sequences into cyclic peptides [48], or replacing the hydrogen-bonding groups with covalent bonds in order to stabilize the turns [49–56]. Benzodiazepines have also been used as turn mimetics [57–59] (In fact, the pioneering work of Ripka et al. [58–59] showed a clear geometrical correspondence between substituent positions on benzodiazepine scaffolds and the orientation of side chains in classical β-turns). Many of the reverse-turn mimics described in the literature, however, particularly the polycyclic systems, require multistep syntheses that severely limit the practical possibilities for selective side-chain incorporation. Takeuchi and Marshall [43] described theoretical calculations that suggest the simple incorporation of Pro-D-Pro-NMe-AA (AA = amino acid other than Gly) into a peptide sequence will stabilize a β-turn with easily accessible side-chain functionality in the $i + 2$ position. The availability of chimeric proline analogs [12, 13, 60–63], or pipecolic acid analogs [64] where side chain functional groups have been

stereoselectively attached to the two ring systems, suggest the preparation of analogs of D-Pro-NMe-AA and Pro-D-NMe-AA, or their pipecolic analogs, that contain side chain functional groups at all positions in the turn.

The availability of other rigid conformational templates that are synthetically accessible for chiral side-chain placement to constrain the conformation of peptides in various conformational states would be extremely useful. Useful constrained scaffolds should satisfy the following three requirements: (i) they should possess only one 3D structure (or only a few well-determined possible structures), (ii) they should be reasonably easy to synthesize in chiral form, and (iii) they should be able to uniquely position the peptide side chains (the recognition elements believed to transfer most information during the peptide-receptor interaction). Pentaazacrowns, when complexed with a metal, are excellent candidates for such conformational templates, as they are relatively rigid structures, relatively easily synthesized by reduction of the amide bonds from precursor cyclic peptides [65], and have many synthetically accessible functional groups from amino acid synthons for chiral side-chain placement. Extensive experimental studies [65–72] on the complexes of PACs as superoxide dismutase mimetics with therapeutic applications have been reported by Riley et al. What, however, is the structural basis for considering metal complexes of azacrowns as potential peptidomimetics? If we look at a peptide structurally, we can divide it into units that go from one C_α atom to the next C_α. Each such unit is a planar rigid group due the partial double-bond character of the *trans*-amide group with known bond distances and bond angles. The relative orientation of adjacent peptide groups (Figure 1) is determined by two degrees of freedom; rotation around the NH–C_α bond and the C_α–C=O bond between the two amides, phi (ϕ) and psi (ψ), respectively. Since the peptide units are effectively rigid groups linked by covalent bonds at the C_α atoms, the only degrees of freedom are rotations around these bonds. Thus, the distance between the two C_α atoms remains fixed (as the two C_αs are on the axes of rotation). In peptides, the C_α to C_α distance measures approximately 3.85 Å for the *tran*-amide. With the exception of amides involving N-methyl-amino acids such as proline, *cis*-amide bonds are generally not observed in peptides. The C_α to C_α distance measures approximately 2.90 Å for the *cis*-amide. One can isolate one unit of the turn, reduce the amide bond, and introduce a new torsional degree of freedom, rotation around the new CH_2–NH bond. A distance range of 2.95 to 3.95 Å was calculated between the carbon atoms of the azacrown unit corresponding to the C_α atoms of two consecutive amino acids of a peptide using systematic search in SYBYL [73]. Thus, reduction of the amide bond dramatically increases the possible distances between the atoms that carry the side chains by the new torsional degree of freedom as well as the concomitant changes in bond lengths and bond angles. If we do the same calculation between adjacent nitrogen atoms, we get a distance range of 2.88 to 3.87 Å. Complexation with the metal, however, restricts the positions of adjacent nitrogens in the azacrown structure (2.70 to 2.90 Å) and, thereby, the possible distances of the carbons corresponding to the C_α atoms in these complexes. The distance measured between atoms (corresponding to the C_α to C_α in peptides) in the crystal structures of the macrocyclic ligands when complexed to the three metals (Mn, Cd and Fe), ranges from 3.60 to 3.97 Å, overlapping the fixed C_α to C_α distance (3.85 Å) in peptides with *trans*-amide bonds. This provides a relatively simple explanation as to why metal complexes of pentaazacrowns may effectively mimic peptide structures.

This study evaluates the potential of metal complexes of chiral pentaazacrowns (PAC) as β-turn mimics. Due to the limited flexibility of the pendant chiral side groups in these metal complexes, we can elicit information about the receptor-bound conformation from their binding. We examined 11 PAC crystal structures [67, 74] (courtesy of Dr. Dennis P. Riley, MetaPhore Pharmaceuticals, Inc.) with different substitution patterns complexed with 3 different metals (Mn, Fe, Cd) as a prototypical database of potential side-chain orientations. It is obvious that complexation with different metals will potentially induce different conformations of a particular azacrown scaffold. The lack of parameterization of transition metals for force field calculations, despite the recent development of an accurate force field describing metal binding including d-orbitals by Carlsson and Zapata [75, 76], precludes a thorough theoretical study of the potential energy surface of such complexes at this time. Thus, we have restricted this study to a simple geometrical comparison between the experimental data for PAC complexes and the side-chain orientations seen in classic β-turns. The FOUNDATION program [77] was used to overlap the C_α-C_β vectors of the corresponding ideal β-turn side-chains to all possible leaving groups of the PAC complexes. When we compared the relative orientations of the chiral

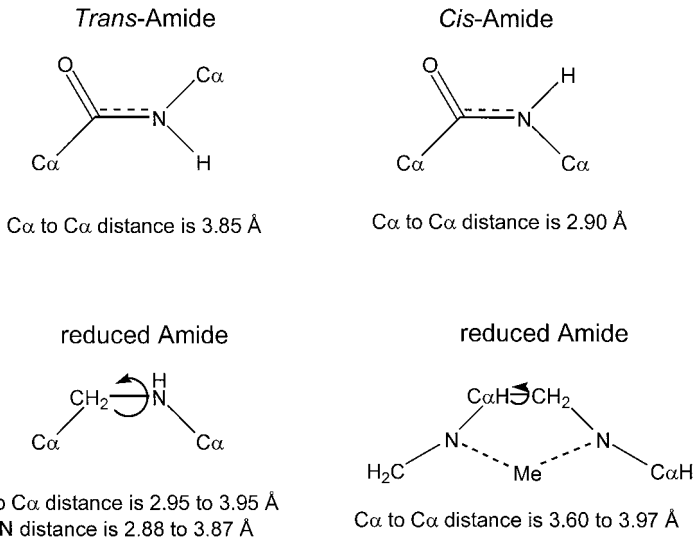

Figure 1. Fixed distances between carbon-alphas in peptides and impact of amide bond reduction and subsequent metal complexation on distances.

side chains, a strong overlap of the bonds (between about 0.1 Å to about 0.5 Å RMS for 3 residues, in most cases, and up to about 1 Å RMS for 4 residues in a limited number of comparisons) was observed. Such metal complexes may lack biological activity as a peptidomimetic due to the lack of spatial overlap of all four side chains; however, if only three peptide side chains are needed for receptor recognition and/or binding, the metal complexes should show biological activity.

Methods

Computational studies were undertaken to evaluate the ability of the designed system to adopt the desired β-turn conformation. A capped tetraalanine peptide, Ac-Ala_4-methylamide, was set to the classical torsion angles associated with the different classes of β-turn types (Table 1). These structures were generated by constraining the backbone angles in residues $i+2$ and $i+3$ to be close to the ideal values and minimizing with SYBYL [73] using the AMBER all-atom force field [78], followed by relaxation of the constraints and further minimization [42, 43], and was used to locate a local minimum near the ideal values for classic β-turns. Table 1 shows the dihedral angles of 10 classes of ideal beta-turns. The dihedral angles and other measurements of our modeled β-turns after minimization are shown in Table 2.

Table 1. Ideal β-turns

Class	ϕ_2	ψ_2	ϕ_3	ψ_3
Type I	−60	−30	−90	0
Type I'	60	30	90	0
Type II	−60	120	80	0
Type II'	60	−120	−80	0
Type III	−60	−30	−60	−30
Type III'	60	30	60	30
Type V	−80	80	80	−80
Type V'	80	−80	−80	80
Type VIa	−60	120	−90	0
Type VIb	−120	120	−60	0

Ideal torsion values for minimization from: Creighton, Thomas E.: Proteins: Structures and Molecular Principles. Table 6–5, page 237. Hutchinson, E. G. and Thornton, J. M.: A revised set of potentials for beta-turn formation in proteins. Protein Science, December 1994.

The 11 PAC compounds used in this study are shown in Figure 2. The following structures can be found in the Cambridge Structural Database[1]: (2) as NAYSEL, (4) as TOJVAP, (6) as PIHWEI, (7) as NAYSAH, (9) as RUGZOI, and (10) as PURWUU. The other 5 structures are not yet available from the Cambridge Structural Database, but the coordinates

[1]These data can be obtained free of charge via www.ccdc.cam.ac.uk/conts/retrieving.html (or from the CCDC, 12 Union Road, Cambridge CB2 1EZ, UK; fax: +44 1223 336033; e-mail: deposit@ccdc.cam.ac.uk)

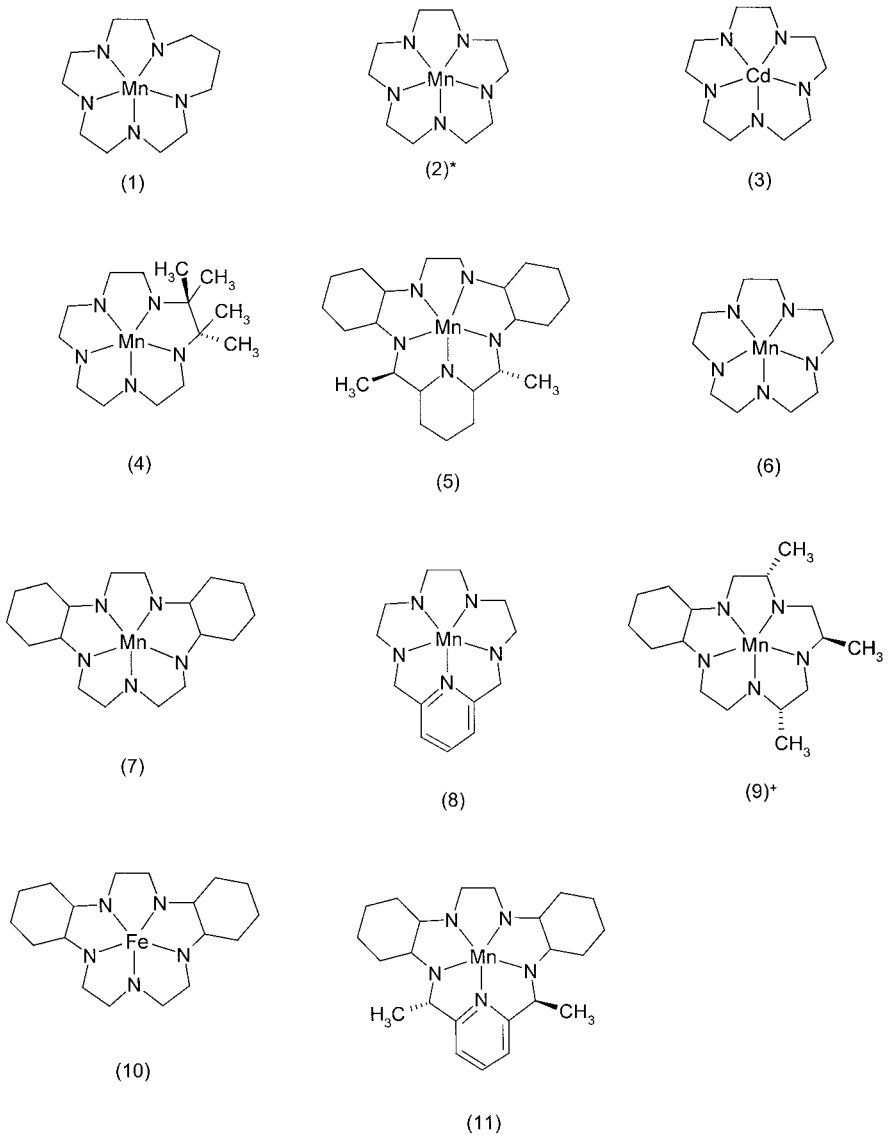

Figure 2. Structures of the 11 pentaazacrown-metal complexes. All macrocyclic ligands are capped in the axial positions by two trans-chloro ligands, unless otherwise noted. *This complex is the bis(nitrato) derivative of (6), which crystallized as the six-coordinate nitrato nitrate complex. +This complex has only one axial chloride.

of crystal structures of the Cd(II) complex (3) [68] and the Mn(II) complex (11) [66] are published. Thus, only coordinates of complexes 1, 5 and 8 are not easily accessible. The iron complexes of the pentaazacyclopentadecane ligands have a very low $Fe^{II/III}$ redox potentials resulting in Fe^{II} complexes that are readily oxidized and very unstable in air. Consequently, for reasons of stability and ease of handling, the crystal structures of the Fe^{III} complexes of the pentaazacyclopentadecane ligands were determined [67]. The crystal structures as would be expected for small molecules all have a high resolution (less than 1.0 Å). The estimated standard deviation (esd) of the unit cells are all given in the thousandths place, the Goodness-of-Fit are all close to 1.0, and R-factors are all less than 5%.

The minimized structures of the turns and the crystal structures of the pentaazacrowns (PAC) were modeled in SYBYL and the coordinates converted from Cartesian space to a distance space matrix, retaining the interatomic distances as a function of atom pairs. The FOUNDATION program [77], that uses a clique-finding algorithm to search the three-dimensional

Table 2. Modeled β-turns after minimization

Class	ϕ_2	ψ_2	ϕ_3	ψ_3	ω_2	ω_3	Distance $C\alpha_1$-$C\alpha_4$	Distance HB (Å)*
Type I	−59.8	−29.6	−90.4	0.1	178.1	179.9	4.499	1.629
Type I'	59.2	29.3	89.0	−0.1	175.2	175.8	4.990	1.631
Type II	−59.9	120.6	80.2	0.5	179.2	−179.2	4.712	1.628
Type II'	59.5	−119.7	−80.4	0.3	172.3	−176.5	4.291	1.712
Type III	−59.9	−30.1	−61.1	−30.4	177.4	−176.5	5.003	2.116
Type III'	59.6	30.2	60.2	30.1	183.6	183.4	5.072	1.958
Type V	35.8	53.1	54.3	30.8	−176.9	179.8	5.268	1.642
Type V'	67.2	−72.6	−106.7	56.6	178.6	−176.1	5.743	4.111
Type VIa	−61.1	121.6	−92.5	0.0	−22.7	168.9	4.383	2.940
Type VIb	−121.3	122.5	−63.8	−1.3	−18.5	−169.2	4.112	3.437

*HB Distance is the distance from the carbonyl oxygen of residue i to the amide hydrogen of residue $i+3$.

distance-geometry database for a user-defined query, was used to retrieve the hits as well as the many near-misses. Finally, all candidate combinations were evaluated for query equivalence.

In the FOUNDATION program, potential matches are retrieved by systematically superimposing each query element upon every atom of the structure being processed. The area around each element is scanned for other query elements with a user-specified distance range (or error margin), creating a hollow sphere. Any atom within the thick wall of the hollow sphere is included as a possible candidate. Thus, the user-specified error margin influences the number of atoms chosen. The constraints perform two major functions: (1) screening and removing query candidates that fail to meet user specifications, drastically reducing the number of combinations that must be checked, and (2) acting as a filter to ensure that the most relevant candidates for the system are returned. Other subset constraints allow the user to specify particular atom types and bond-atom constraints. The number of combinations varies according to the size of the query, the constraints placed on the query, and the number of matching elements requested. The ability of FOUNDATION to retrieve partial hits makes this tool indispensable for this application. Query specifications can contain any number of atoms or bonds provided that adequate constraints are given to reduce the computational load. The constraints are: (1) bonded vs. isolated atom distinction, (2) atom type designation, (3) definition of subsets with occupancy specification ($>$, $=$, $<$ X atoms), (4) RMS fit, (5) active-site volume accessibility of atoms linking query elements, (6) number, atom type, and cyclic structure constraints for atoms linking pharmacophoric elements, and (7) automatic error boundary adjustment.

The hits and near-misses matching our query were examined for reasonable line-up of the peptide backbone with the pentaazacrown of the complex. If the metal atom did not fall near the center of the β-turn it was discarded as a possible candidate. For example, molecule (10) aligned with β-turn type III', but the metal ion in the center of the pentaazacrown aligned with an atom in the backbone of the peptide. This alignment was dropped from further consideration. The molecules remaining were then evaluated for alignment with a leaving group on the PAC with the side chains of the β-turns. Candidates for leaving groups were all of the hydrogens on the carbon and nitrogen atoms of the PAC. Measurements were taken of (1) the distance between the C_α of the β-turn residue with the matching atom of the PAC, (2) the C_β atom with matching atom, and (3) the angle between the matching bond pairs. These measurements are illustrated in Figure 3.

Results and discussion

Table 1 shows the ϕ_2, ψ_2, ϕ_3, and ψ_3 values for the 10 classes of ideal β-turns. Table 2 shows the ϕ_2, ψ_2, ω_2, ϕ_3, ψ_3, ω_3, distance between the C_α of the first residue (i) and the C_α of the fourth residue ($i+3$) ($C_{\alpha1}$-$C_{\alpha4}$ distance), and the distance from the carbonyl oxygen of residue i to the amide hydrogen of residue $i+3$ (HB distance). A comparison of Tables 1 and 2 shows that the ϕ_2, ψ_2, ϕ_3, and ψ_3 are very close in values for almost all of the 10 classes of ideal β-turns. The

Table 3. Angle between the vectors (C_α to C_β bond vs. metal complex of PAC; C to methyl bond of β-turn), the C_α and C_β distance difference for each match of the residues in the reverse turn, and the RMS overlap of the residues.

Turn	Ligand	Angle (degrees)				Cα Distance (Angstroms)				Cβ Distance (Angstroms)				RMS (Angstroms)			
		j	*j*+1	*j*+2	*j*+3	*j*	*j*+1	*j*+2	*j*+3	*j*	*j*+1	*j*+2	*j*+3	*j*	*j*+1	*j*+2	*j*+3
I	(2)	9.6	15.6	22.3	41.0	0.14	0.39	0.62	0.76	0.15	0.52	0.27	1.23	0.14	0.46	0.48	1.02
	(10)	7.3	10.0	81.9	21.4	0.18	0.26	1.67	0.28	0.05	0.21	1.65	0.44	0.13	0.24	1.66	0.37
	(11)	6.0	2.3	23.8	3.3	0.20	0.45	0.76	0.21	0.00	0.26	0.76	0.23	0.16	0.37	0.76	0.22
I'	(1)	16.0	15.4	–	13.4	0.20	0.65	–	0.56	0.26	0.57	–	0.49	0.23	0.61	–	0.53
	(2)	16.5	–	4.2	25.9	0.49	–	0.42	0.54	0.07	–	0.51	0.25	0.35	–	0.47	0.42
	(3)a	14.5	27.3	–	13.6	0.26	0.51	–	0.39	0.15	0.70	–	0.53	0.33	0.38	–	0.64
	(3)b	22.1	–	5.5	27.5	0.41	–	0.44	0.62	0.23	–	0.31	0.67	0.21	–	0.61	0.47
II	(1)	9.3	25.4	53.0	–	0.22	0.30	0.77	–	0.00	0.42	0.64	–	0.16	0.37	0.71	–
	(4)	13.8	8.8	36.1	17.5	0.29	0.08	1.11	0.32	0.08	0.31	0.42	0.18	0.22	0.23	0.84	0.26
	(6)	9.0	30.5	18.1	21.0	0.23	0.12	1.14	0.50	0.02	0.84	1.03	0.48	0.16	0.60	1.09	0.49
II'	(1)	4.0	10.5	11.9	17.7	0.06	0.33	0.30	0.44	0.06	0.11	0.18	0.79	0.06	0.24	0.25	0.64
	(2)a	6.2	7.3	5.3	–	0.16	0.23	0.24	–	0.01	0.12	0.23	–	0.11	0.18	0.24	–
	(2)b	6.1	16.9	11.0	–	0.01	0.46	0.40	–	0.16	0.13	0.23	–	0.11	0.34	0.32	–
	(2)c	0.4	20.0	44.1	–	0.01	0.37	0.85	–	0.02	0.43	0.37	–	0.01	0.40	0.65	–
	(3)a	3.3	20.6	7.0	15.6	0.11	0.71	0.31	0.29	0.15	0.17	0.25	0.38	0.13	0.52	0.28	0.34
	(3)b	0.1	17.8	3.2	17.8	0.05	0.54	0.32	0.61	0.06	0.10	0.36	0.56	0.05	0.39	0.34	0.59
	(3)c	12.8	17.1	30.4	24.2	0.32	0.68	0.92	1.35	0.03	0.41	0.26	0.71	0.23	0.56	0.68	1.08
	(6)	3.2	16.1	24.5	–	0.06	0.63	0.71	–	0.09	0.24	0.24	–	0.08	0.48	0.53	–
	(7)	5.8	13.4	14.9	–	0.14	0.41	0.44	–	0.02	0.11	0.20	–	0.10	0.30	0.34	–
	(8)a	3.8	18.7	16.7	–	0.00	0.67	0.65	–	0.10	0.28	0.34	–	0.07	0.46	0.47	–
	(8)b	3.5	17.5	15.0	–	0.10	0.61	0.58	–	0.00	0.23	0.31	–	0.07	0.51	0.52	–
	(10)a	–	8.0	20.0	25.0	–	0.16	0.71	0.83	–	0.08	0.44	0.30	0.13	0.59	0.62	–
	(10)b	2.6	9.7	60.1	17.8	0.00	0.32	0.66	0.85	0.07	0.22	0.93	0.52	0.05	0.28	0.81	0.70
III	(2)	13.9	32.3	18.9	27.3	0.19	0.37	1.81	0.55	0.20	0.72	2.19	0.43	0.20	0.57	–	0.49
III'	(1)	4.8	–	12.2	6.5	0.29	–	0.62	0.49	0.26	–	0.46	0.42	0.28	–	0.54	0.45
	(2)	10.6	32.7	20.6	–	0.19	0.52	0.56	–	0.28	0.41	0.36	–	0.24	0.47	0.47	–
	(3)a	4.0	56.9	22.4	–	0.27	0.68	0.36	–	0.12	0.70	0.60	–	0.21	0.69	0.49	–
	(3)b	22.7	31.1	–	29.2	0.27	0.56	–	0.66	0.20	0.41	–	0.39	0.24	0.49	–	0.54
	(4)	7.6	3.2	35.9	–	0.13	0.56	0.44	–	0.16	0.25	0.72	–	0.15	0.43	0.60	–
V	(3)a	41.8	13.8	23.0	10.3	0.98	0.18	0.66	0.59	2.07	0.22	0.44	0.47	1.62	0.20	0.56	0.54
	(3)b	2.0	19.8	13.3	13.0	0.15	1.42	0.36	0.13	0.15	1.61	0.17	0.24	0.15	1.52	0.28	0.19
	(3)c	11.3	10.9	7.4	58.1	0.24	2.64	0.21	0.79	0.14	2.69	0.02	0.72	0.20	–	0.15	0.75
V'	(2)	10.0	43.3	9.6	–	0.17	0.59	0.32	–	0.12	0.67	0.13	–	0.15	0.63	0.25	–
	(3)	14.0	19.1	19.2	–	0.29	0.48	0.65	–	0.09	0.42	0.40	–	0.22	0.45	0.54	–
	(6)	–	9.7	34.6	29.7	–	0.17	0.08	0.58	–	0.11	0.88	0.54	–	0.14	0.63	0.56
	(8)a	–	8.0	42.8	27.1	–	0.21	0.62	0.52	–	0.00	0.54	0.26	–	0.15	0.58	0.41
	(8)b	–	7.9	43.9	26.0	–	0.21	0.68	0.51	–	0.01	0.51	0.27	–	0.15	0.60	0.41
	(9)a	8.9	11.8	42.2	34.8	2.29	0.52	0.40	0.69	2.73	0.02	0.72	0.24	–	0.37	0.58	0.52
	(9)b	–	8.6	46.8	26.9	–	0.01	0.58	0.55	–	0.49	0.62	0.37	–	0.35	0.60	0.47
	(10)	–	7.3	43.1	27.5	–	0.03	0.74	0.53	–	0.17	0.44	0.28	–	0.12	0.61	0.42
VIa	(1)	0.1	17.3	5.6	16.4	0.14	0.24	0.31	2.54	0.15	0.58	0.22	2.81	0.15	0.45	0.27	–
	(3)	18.2	12.7	15.5	9.6	0.39	0.52	0.37	2.00	0.10	0.25	0.57	2.00	0.29	0.41	0.48	–
VIb	(2)a	0.6	28.7	33.5	17.0	0.13	1.40	0.92	0.66	0.12	1.79	0.35	0.36	0.13	1.61	0.69	0.53
	(2)b	9.0	20.3	35.5	50.6	0.27	0.61	0.44	0.99	0.03	0.10	0.61	1.51	0.19	0.44	0.53	1.28
	(2)c	27.7	20.5	38.4	5.5	0.59	0.60	0.51	2.08	0.19	0.14	0.54	2.11	0.44	0.44	0.53	–
	(2)d	7.7	19.5	34.3	33.7	0.06	2.25	0.69	0.57	0.26	2.71	0.36	0.46	0.19	–	0.55	0.52
	(3)	15.7	34.7	21.1	–	0.18	0.54	0.32	–	0.25	0.41	0.32	–	0.22	0.48	0.32	–

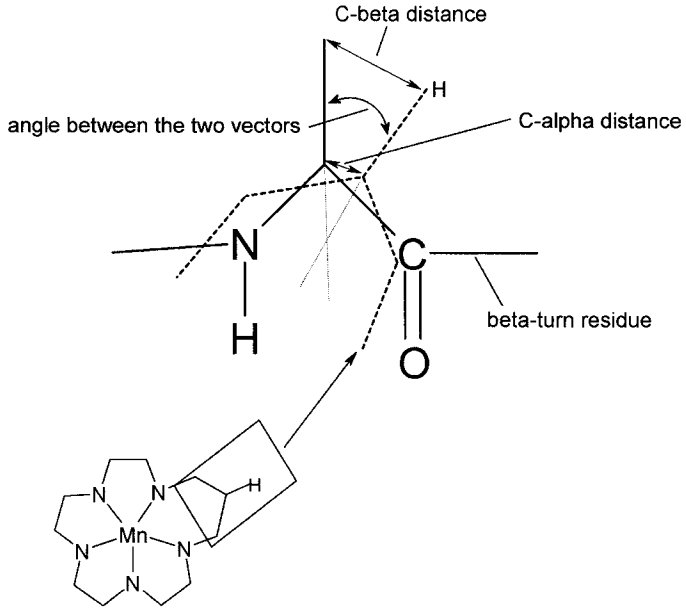

Figure 3. Measurements taken on the residues of the beta-turns to the hydrogens of the ligands. Measurements were taken of (1) the distance between the C_α of the β-turn residue with the matching atom of the PAC, (2) the C_β atom with matching atom, and (3) the angle between the matching bond pairs.

angles measured after relaxation of the constraints and minimization for turn types V and V' are not as close to the ideal β-turns as the other turn types. The other measurements are given to give a sense of the different types of ideal β-turns. The most open turn is turn type V' defined by a $C_{\alpha 1}$-$C_{\alpha 4}$ distance of 5.74 Å and a HB distance of 4.11 Å, followed by type V (based on the $C_{\alpha 1}$-$C_{\alpha 4}$ distance). The HB distance of V' and VIb are greater than the distance expected for a hydrogen bond, thus, these turns are characterized by a lack of hydrogen bonding between the carbonyl oxygen of residue *i* to the amide hydrogen of residue $i + 3$.

After analysis with FOUNDATION, distances between atoms, angles between bonds, and RMS values were determined. The angle between the vectors (bonds) and the C_α distance and C_β distance for each match is given in Table 3. The RMS values are also given in Table 3. However, if the measured value of the C_α or C_β distance was greater than 2 Å, the RMS was not reported. The number of β-turns hit by the molecules and the types of theses turns, as well as the total number of hits of each molecule, is shown in Table 4. The average and all the distances of the bonds between the nitrogen of the azacrown and the metal ion of the macrocyclic ligand for each molecule are given in Table 5. The best fit of any molecule to a classical turn is complex (3) to β-turn type II' (Figure 4). The RMS fit of the *i*th, $i + 1$st, $i + 2$nd, and $i + 3$rd C_α to C_β vector is 0.129, 0.515, 0.278, and 0.338, respectively, indicating that a high degree of similarity existed in the turn region with the PAC in terms of potential side-chain mimicry for all four-residue vectors. β-turn type II' also had two other complexes with a four-residue match (Figure 6 and 9a).

Interestingly, the two complexes with the most hits are (2) and (3), which have nearly the shortest and longest average N-to-metal ion distances. The shortest and longest average distance, molecules (10) and (1) respectively, were also popular β-turn hits with 4 and 5 different β-turns hit.

The ideal beta-turn type I found hits with molecules (2), (10), and (11). Molecule (2) hit the *i*th $i+1$st, and $i + 2$nd positions with reasonable distance of C_α being less than 0.7 Å. Angles between those vectors were all less than 30°. The fourth vector shows the C_α atoms off by 0.76 Å. The angle between the vectors is 41.0°. Molecule (10) shows a tight fit for residues *i*, $i + 1$st and $i + 3$rd. The third vector, $i + 2$nd, essentially has no overlap. Molecule (11) shows good overlap between the same residues as molecule (10). However, the $i + 2$nd residue on molecule (11) is off by over 0.7 Å for both the C_α and C_β, but the angle is still under 30°. Both vectors point in approximately the same direction, but this residue on molecule (11)

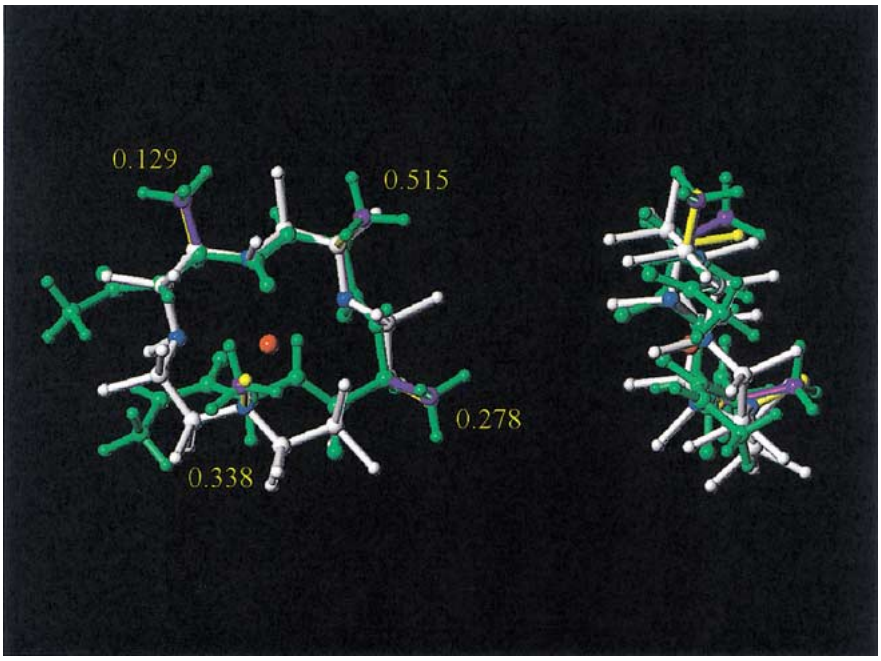

Figure 4. Beta-turn type II' aligned with complex (3). Red atom indicates cadmium; numbers indicate rmsd between α–β vectors.

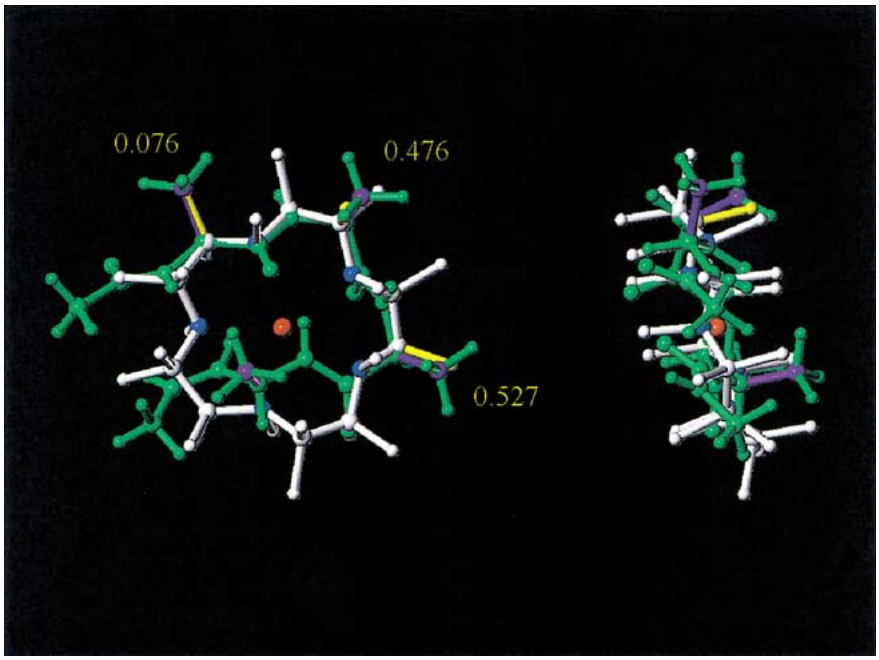

Figure 5. Beta-turn type II' aligned with complex (6). Red atom indicates manganese; numbers indicate rmsd between α–β vectors.

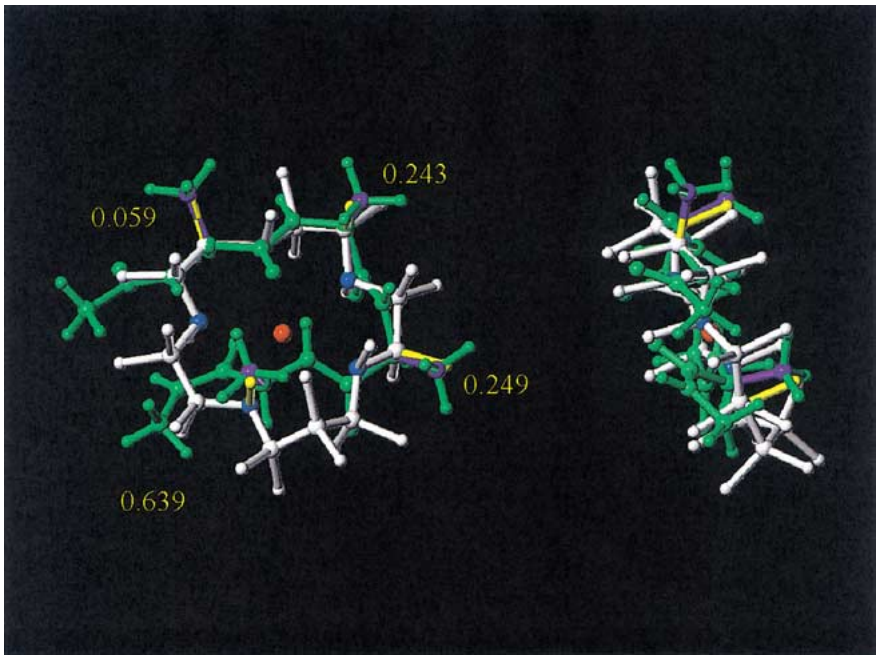

Figure 6. Beta-turn type II' aligned with complex (1). Red atom indicates manganese; numbers indicate rmsd between α–β vectors.

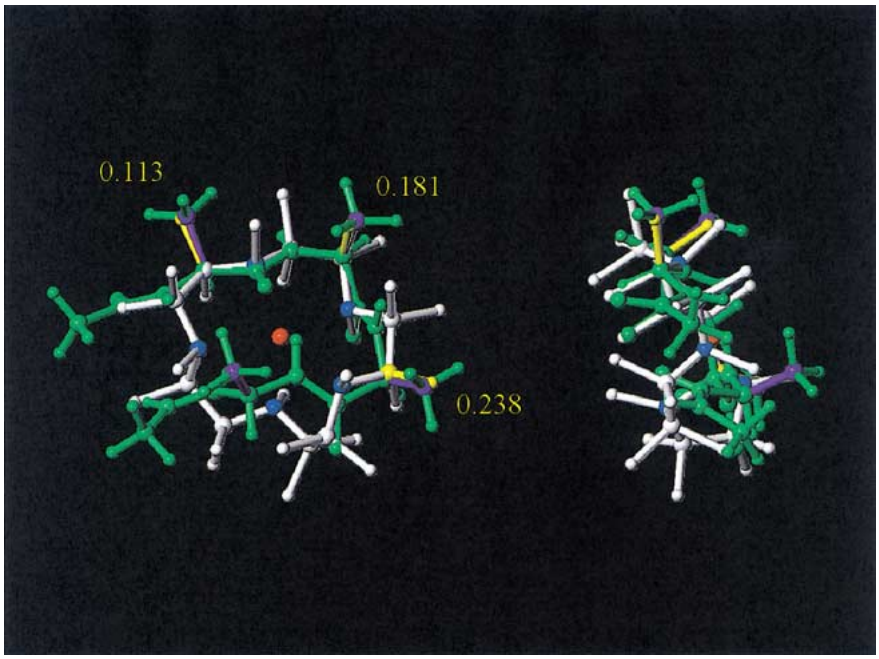

Figure 7. Beta-turn type II' aligned with complex (2). Red atom indicates manganese; numbers indicate rmsd between α–β vectors.

Table 4. Number of hits and type of β-turn hit for each molecular complex.

Molecule #	No. of Turns Hit	Turns Hit	Number of Hits
(1)	5	I', II, II', III', VIa	5
(2)	7	I, I', II', III, III', V', VIb	12
(3)	7	I', II', III', V, V', VIa, VIb	13
(4)	1	II	1
(5)	0	–	0
(6)	3	II, II', V'	3
(7)	1	II'	1
(8)	2	II', V'	4
(9)	1	V'	2
(10)	4	I, II', III', V'	5
(11)	1	I'	1

Table 5. Distance between nitrogens of azacrown and metal ion (all Mn except 3 (Cd) and 10 (Fe)).

Molecule #	Average N-Metal	Lengths: N-Metal (shortest to longest)
(1)	2.42[a]	2.31, 2.34, 2.34, 2.53, 2.56
(2)	2.28[b]	2.27, 2.28, 2.28, 2.28, 2.31
(3) - Cd	2.415[c]	2.35, 2.38, 2.41, 2.45, 2.48
(4)	2.33	2.31, 2.32, 2.32, 2.34, 2.38
(5)	2.33	2.23, 2.30, 2.35, 2.37, 2.38
(6)	2.36	2.26, 2.27, 2.40, 2.41, 2.44
(7)	2.33	2.31, 2.31, 2.32, 2.34, 2.37
(8)	2.33	2.27, 2.34, 2.34, 2.34, 2.34
(9)	2.34	2.31, 2.33, 2.35, 2.36, 2.36
(10) - Fe	2.27[d]	2.25, 2.26, 2.28, 2.28, 2.29
(11)	2.32	2.24, 2.30, 2.31, 2.35, 2.41

[a]Longest Mn average N-metal distance.
[b]Shortest Mn average N-metal distance.
[c]Cd average N-metal distance similar to longest Mn average N-metal distance.
[d]Fe average N-metal distance similar to shortest Mn average N-metal distance.

is set out further away from the turn. This may line-up with longer side-chain residues as the flexibility of the side chain may compensate during receptor interaction, but the utility as relatively rigid mimetics would be compromised.

For ideal beta-turn type I', 4 different molecules from the database matched the query. There were two hits by molecule (3). These two hits were on different atoms of the molecule and matched different combinations of residues. Molecules (1) and (3) matched residues i, $i+1$st, and $i+3$rd. Molecules (2) and (3) hit residues i, i + 2nd, and i + 3rd. Molecule (1) was the best line-up for residues i, $i+1$st, and $i+3$rd. Molecule (2) was the best line-up for residues i, i + 2nd, and i + 3rd.

Beta-turn type II had three molecules match the query. Molecule (4) hit all four residues and is by far the best fit to this turn. Molecule (6) had good line-up with all but the third residue (i + 2nd), yet had a reasonable line-up with this residue.

Beta-turn type II' was very popular having 13 hits from 7 different molecules (Figures 4–9), not all are shown. The best overall fit was from molecule (3) matching all four residues with an RMS ranging from 0.129 to 0.515 Å for the vector overlap (Figure 4). Molecule (1) lined up all four residues (Figure 6) with RMS values, from 0.059 to 0.639 Å, similar to these given for the line-up with molecule (3). Molecule (10) also had a good line-up with all four residues (Figure 9a & 9b), but the trans-cyclohexane rings may

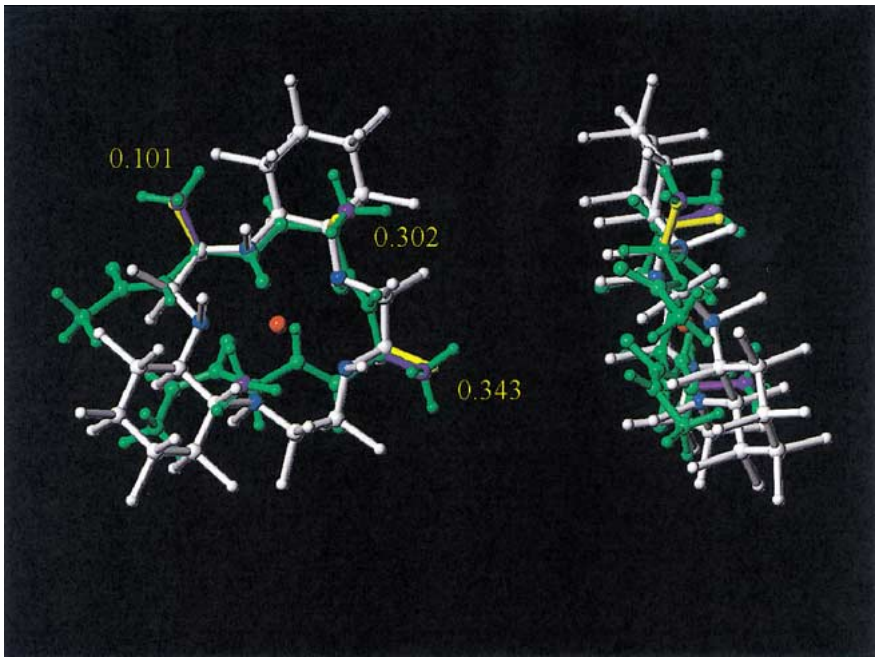

Figure 8. Beta-turn type II' aligned with complex (7). Red atom indicates manganese; numbers indicate rmsd between α–β vectors.

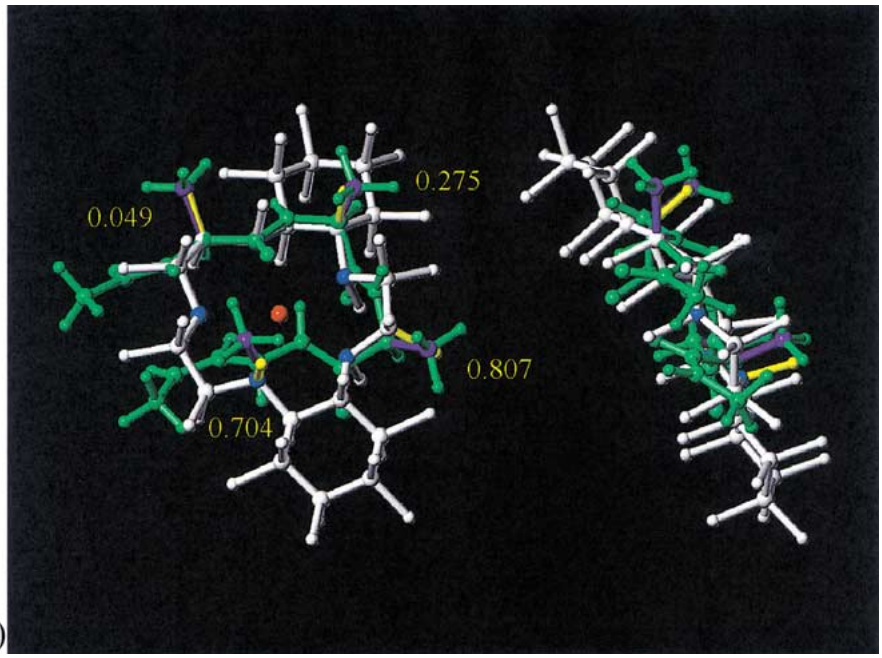

a)

Figure 9a. Beta-turn type II' aligned with complex (10). Red atom indicates iron; numbers indicate rmsd between α–β vectors.

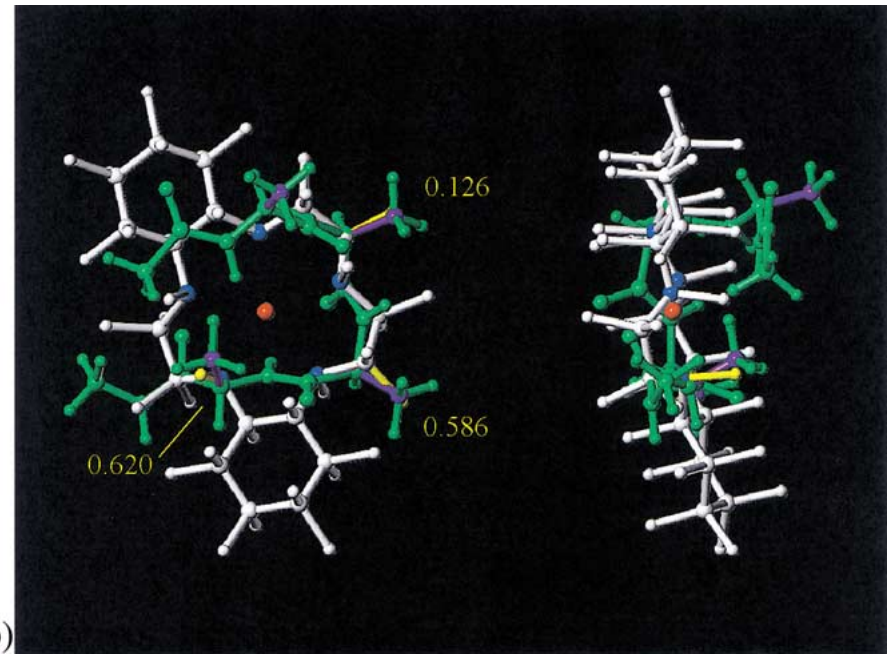

Figure 9b. Beta-turn type II' aligned with complex (10). Red atom indicates iron; numbers indicate rmsd between α–β vectors.

cause problems sterically. If you recall, molecule (2) is the bis(nitrato) derivative of molecule (6). Comparing the alignment of these molecules with ideal β-turn II', we can see that they line-up with the same residues (*i*, $i+1$, and $i+2$) but in slightly different ways. Looking at the side view of the two figures shows residue $i+3$ off by a greater distance in molecule (2) than in molecule (6), but RMS values show a smoother line-up of the three residues. [t!]

Beta-turn type III had only one hit. Molecule (2) aligned with residues *i*, $i+1$st, and $i+3$rd. There was no alignment from any molecule to residue $i+2$nd in combination with another position.

Beta-turn type III' found 6 matches, but molecule (10) did not line-up with the backbone of the turn. Thus, molecule (10) was not included in this analysis. Once again, molecule (3) had two matches, but aligned different residues. No molecules matched all four residues together, but all combinations of three residues were matched at least once, except the second, third, and fourth residues ($i+1$st, $i+2$nd, $i+3$rd).

Beta-turn type V has three matches from only one molecule. It is, however, the same molecule that hit 7 out of the 10 turn types, molecule (3). There is a possibility of aligning all 4 residues. Residue I for match (3)a was off by 0.98 Å (for C_α) and 2.07 Å (for C_β) and by 41° for the angle between the vectors. Residue $i+1$ for match (3)b was off by 1.4 to 1.6 Å, but the angle between the vectors was off by less than 20°.

Beta-turn type V' has 8 hits from 6 different molecules. The only two combinations of hits were residues *i*, $i+1$st, and $i+2$nd and residues $i+1$st, $i+2$nd, and $i+3$rd. Residues *i* and $i+3$rd are not hit at the same time.

Beta-turn type VIa had only two hits and only residues *i*, $i+1$st, and $i+2$nd were hit for the two molecules. Residue $i+3$rd had no alignment in combination with another residue.

Beta-turn type VIb had 5 hits from two molecules. The closest to a four-residue fit was from molecule (2). This is the same molecule that hit four times. Different atoms were aligned to the turn vectors in each hit. Molecule (3) matched residues *i*, $i+1$st, and $i+2$nd.

Overall, peptidomimetics based on Molecule (3) is going to easily mimic the ideal beta-turn type II', but is not able to distinguish it from a Type V turn. Molecule (2) will best mimic a Type VIb turn. Molecule (4) peptidomimetics will likely indicate a Type II turn. Scaffolds utilizing Molecule (1) will likely bind to sites with preferences for a Type II' turn.

It is interesting to compare the conformational impact on changing the metal used for complex formation with the same ligand. In the database of 11 complexes used for in this study, there are two examples available for such a comparison. First, com-

plexes (3) with cadmium and (6) with manganese utilize the same unsubstituted pentaazacrown ligand with two chlorides as axial ligands. Figures 4 and 5 show molecules (3) and (6), respectively, lined-up with ideal β-turn II'. Note that complex (3) aligns all four residues while complex (6) aligns only three of the residues. The question then is, 'What is the difference in the two metals used which allows this difference in the alignment with the same β-turn?' If we compare the molecules with structural similarity and different metal ions we can, perhaps, answer this question. Looking at Table 6 we see that the average distance between the nitrogens of the ligand and the metal is 2.42 Å for the cadmium complex and 2.36 Å for the manganese complex. In order to compare the distance between the carbon atoms around the ring of the macrocyclic ligand corresponding to the C_α atoms of a peptide, we measured the distance between every carbon atom in the ring with every carbon 3 atoms away. Molecule (6) measures an average distance of 3.70 Å with a standard deviation of 0.12 Å. Molecule (3) has an average distance between carbon atoms (3 atoms away) of 3.72 Å with a standard deviation of 0.14 Å. The distance between the nitrogen atoms of molecule (6) averages 2.80 Å with a standard deviation of 0.07 Å, while the distance between nitrogen atoms of molecule (3) averages 2.86 Å with a standard deviation of 0.01 Å. These numbers are not surprising if we refer to the periodic table. Cd has a much higher nuclear charge (Z), a higher period (n), and a greater number of core electrons. These are competing effects, but n has the strongest effect, so the ionic radius of Cd is larger than Mn, more substantially larger than the ionic radius difference between Fe and Mn. Complexes (7) with iron and (10) with manganese utilize a pentaazacrown ligand with two fused cyclohexyl rings and two chloride atoms as ligands. The alignment of complexes (7) and (10) with ideal β-turn type II' is shown in Figures 8 and 9, respectively. Line-up of residues i, $i + 1$, and $i + 2$ with molecule (7) is shown in Figure 8. The two alignments of molecule (10) with residues i, $i + 1$, $i + 2$, and $i + 3$ and residues $i + 1$, $i + 2$, and $i + 3$ are shown in Figure 9a and 9b, respectively. The average distance (Table 5) between the nitrogens of the ligand and the metal is 2.27 Å for the iron complex and 2.33 Å for the manganese complex. Molecule (7) has an average distance between carbons 3 atoms away of 3.77 Å with a standard deviation of 0.02 Å and an average N-to-N distance of 2.75 Å with a standard deviation of 0.05 Å; while the average carbon to carbon distance for molecule (10) is 3.76 Å with a standard deviation of 0.02 Å and an average N-to-N distance of 2.68 Å with a standard deviation of 0.05 Å. This is also understandable looking at the periodic table. Fe has a slightly higher nuclear charge than Mn, causing a slightly smaller ionic radius. Clearly, different metals will perturb the pentaazacrown in slightly different ways causing angle changes in the positions of the leaving groups on the macrocyclic ligand. What is somewhat surprising is the fact that an increase in the radius of the bound metal ion of 0.06 Å (Cd vs. Mn) does not produce significant changes in the relative positions of the carbons to which one would attach side chains. Future studies with different metals, both experimental and theoretical, will allow us to determine how metals affect the positions and orientations of the leaving groups and should allow more effective use of these metal-complexes as receptor probes and peptidomimetics. It should be emphasized that the comparisons made in this study were on static crystal structures; the potential surfaces for these complexes have not been characterized and their dynamic flexibility remains an issue to be determined.

Molecular flexibility may be an important consideration for binding activity [79]. Mao reported that when molecular flexibility of the octapeptide inhibitor of the aspartyl proteinase from *Rhizopus chinensis*, rhizopuspepsin, was reduced by conformational restrictions on dihedral rotations of the polypeptide, the rigidified molecule could not dissociate in dynamical simulations from the binding pocket of the receptor. This concern is not necessarily general and may reflect the size of the ligand under study; many constrained polycyclic compounds such as benzodiazepine analogs bind with reasonable affinity and rapidity to their receptors. Thus, while the rigidity of some metal pentaazacrowns may limit receptor binding, the flexibility of these complexes should be sufficient in the less constrained cases to allow us to explore this issue. The methodology described here represents a step towards incorporating side-chain orientation into peptidomimetic design by first using conformational templates to generate a hypothesis for the receptor-bound pharmacophore (3D recognition requirements of the side chains by the receptor). Then, one can evaluate the role of molecular flexibility in ligand binding by studying how the rates of dissociation and association are affected by reduced molecular flexibility. Once the 3D arrangement of the side-chain groups are identified and the required molecular flexibility determined, other scaffolds with more desirable drug-like properties could be utilized in the design of

ligands through the use of a number of computer-aided tools [77, 80, 81].

The *in vivo* stabilities of some manganese complexes of pentaazacrowns have been clearly established. Riley et al. reported that Mn(II) complexes with high kinetic stabilities (i.e. low K_{diss}) have high *in vivo* stabilities with good correlation [71] to their *in vitro* measurements. Using cadmium for the metal ion could be very interesting for spectroscopic studies, as the ^{113}Cd chemical shift has been shown to be remarkably sensitive to the types of donor atoms, coordination number and geometry [68]. The Cd(II) and Mn(II) ions possess filled and half-filled d-shells, respectively, and thus the coordination geometry of the complexes are not subject to ligand field effects and have been shown to be stable at physiological pH [82, 83]. The issue of Fenton chemistry and potential generation of hydroxide radicals are relevant for complexes containing iron or copper in any potential therapeutic application. While complexes containing Fe(III) have been found to be stable at physiological pH for months as reported by Zhang et al. [67], the ability of iron in these intact complexes to generate hydroxide radicals has not been ascertained. The need for further *in vivo* testing and thorough evaluation of toxicology for any use of such metal complexes as a pharmaceutical is obvious, but potential problems with ferric complexes cause additional concern.

Conclusions

This study contributes a simple and direct approach to peptidomimetic design. Modeling studies have shown that the potential side-chain orientations of conformations of the limited set of crystal structures of metal complexes of PACs are in close agreement with those of ideal β-turns. Considering the conformation perturbations available from substituent patterns on the pentaazacrown ring, as well as complexation with different metals yet to be thoroughly explored, these results are exceptionally encouraging for developing a two-dimensional library of different chiral PACs complexed with different metals to probe the details of receptor recognition. The minor changes in side-chain orientation with different metals offer an opportunity for subtle optimization of binding not available through conventional organic chemistry. We believe that these systems can serve as useful conformational constraints that, when incorporated in the sequential side-chain motifs of selective bioactive peptides, will yield new conformationally constrained peptidomimetics. Modeling and experimental studies on α-amylase inhibitors and some platelet aggregation inhibitors, which contain the recognition sequence RGD (Arg-Gly-Asp) as their functional motif, with metal complexes of PACs are underway.

These compounds, with fixed side-chain placement and accessible synthetic routes, provide ideal structural probes for applications in combinatorial libraries. Screening analysis from libraries can be used to test for a consistent hypothesis concerning the receptor-bound conformation of the parent peptide. This hypothetical conformation can then be used to select additional classes of modifications (cyclization, new scaffolds, etc.) to be included in further analysis of the receptor-bound conformation. The use of metal complexes of pentaazacrowns as scaffolding devices in peptide sequences should lead to the stabilization of the secondary structure and facilitate the determination of the receptor-bound conformation in combination with the variety of other scaffolds (cyclic pentapeptides, benzodiazapines, etc.) currently in use.

Acknowledgements

The authors acknowledge the support of the NIH (GM53630) for support of this study, and Mr. Bryan A. Keith for his work in minimization of the classical β-turns. They also wish to thank Dr. Dennis Riley of MetaPhore Pharmaceuticals, Inc. for making the crystal structures of PAC-metal complexes (both published and in press) available. Those interested in obtaining such crystal data are advised to contact Dr. Riley directly.

References

1. Marshall, G.R., Curr. Opin. Struct. Biol., 2 (1992) 904–919.
2. Marshall, G.R., Biopolymers (Peptide Sci.), 60 (2001) 246–277.
3. Marshall, G.R., Tetrahedron, 49(17) (1993) 3547–3558.
4. Rose, G.D., L.M. Gierasch, and J.A. Smith, Adv. Protein Chem., 37 (1985) 1–109.
5. Stanfield, R.L., et al., Science, 248(6) (1990) 712–719.
6. Rose, G.D., Nature, 272 (1978) 586–590.
7. Gante, J., Angew. Chem. Int. Ed. Eng., 33 (1994) 1699–1720.
8. Giannis, A. and T. Kolter, Angew. Chem. Int. Ed. Engl., 32 (1993) 1244–1267.
9. Rini, J.M., U. Schulze-Gahmen, and I.A. Wilson, Science, 255(February) (1992) 959–965.
10. Garcia, K.C., et al., Science, 257 (1992) 502–507.
11. Nikiforovich, G.V. and G.R. Marshall, Biochem. Biophys. Res. Commun., 195(1) (1993) 222–228.

12. Plucinska, K., et al., J. Med. Chem., 36(13) (1993) 1902–1913.
13. Kaczmarek, K., et al., in *Peptides: Proceedings of the 13th American Peptide Symposium*, R. Hodges and J.A. Smith, Editors. ESCOM Scientific Publishers, Leiden, (1994) 687–689.
14. Kyle, D.J., et al., J. Med. Chem., 36(10) (1993) 1450–1460.
15. Nikiforovich, G. and G.R. Marshall, Int. J. Pept. Protein Res., 42 (1993) 171–180.
16. Nikiforovich, G.V. and G.R. Marshall, Int. J. Pept. Protein Res., 42 (1993) 181–193.
17. Nutt, R.F., D.F. Veber, and R. Saperstein, J. Am. Chem. Soc., 102(21) (1980) 6539–6545.
18. Brady, S.F., et al., Tetrahedron, 49(17) (1993) 3449–3466.
19. Ball, J.B. and P.F. Alewood, J. Mol. Recog., 3(2) (1990) 55–64.
20. Holzemann, G., Kontakte (Darmstadt), (1991)(2) 55–63.
21. Holzemann, G., Kontakte (Darmstadt), (1991)(1) 3–12.
22. Hanessian, S., et al., Tetrahedron, 53(38) (1997) 12789–12854.
23. Halab, L., F. Gosselin, and W.D. Lubell, Biopolymers, 55(2) (2000) 101–122.
24. Freidinger, R.M., D.S. Perlow, and D.F. Veber, J. Org. Chem., 47 (1982) 104–109.
25. Nagai, U., et al., Tetrahedron Lett., 49(17) (1993) 3577–3592.
26. Lombart, H.-G. and W.D. Lubell, J. Org. Chem., 59(21) (1994) 6147–6149.
27. Hinds, M.G., N.G.J. Richards, and J.A. Robinson, J. Chem. Soc., Chem. Commun., (1988) 1447–1449.
28. Hinds, M.G., et al., J. Med. Chem., 34(6) (1991) 1777–1789.
29. Genin, M.J. and R.L. Johnson, J. Am. Chem. Soc., 114(23) (1992) 8778–8783.
30. Ward, P., et al., J. Med. Chem., 33(7) (1990) 1848–1851.
31. Toniolo, C., et al., Biopolymers, 22 (1983) 205–215.
32. Valle, G., et al., Int. J. Pept. Protein Res., 38 (1991) 511–518.
33. Welsh, J.H., et al., FEBS Lett., 297(3) (1992) 216–220.
34. Zerkout, S., et al., Int. J. Peptide Protein Res., 44 (1994) 378–384.
35. Diaz, H., J.R. Espina, and J.W. Kelly, J. Am. Chem. Soc., 114(21) (1992) 8316–8318.
36. Diaz, H., et al., Tetrahedron, 49(17) (1993) 3533–3545.
37. Tsang, K.Y., et al., J. Am. Chem. Soc., 116(9) (1994) 3988–4005.
38. Bach II, A.C. and L.M. Gierasch, J. Am. Chem. Soc., 107 (1985) 3349–3350.
39. Bach II, A.C. and L.M. Gierasch, Biopolymers, 25 (1986) S175–S191.
40. Chauhan, V.S., et al., Int. J. Pept. Protein Res., 29 (1987) 126–133.
41. Palmer, D.E., et al., J. Am. Chem. Soc., 114(14) (1992) 5634–5642.
42. Chalmers, D.K. and G.R. Marshall, J. Am. Chem. Soc., 117 (1995) 5927–5937.
43. Takeuchi, Y. and G.R. Marshall, J. Am. Chem. Soc., 120(22) (1998) 5363–5372.
44. Sukumaran, D.K., M. Prorok, and D.S. Lawrence, J. Am. Chem. Soc., 113 (1991) 706–707.
45. Zabrocki, J., et al., J. Am. Chem. Soc., 110(17) (1988) 5875–5880.
46. Smith, G.D., et al., Int. J. Pept. Protein Res., 37 (1991) 191–197.
47. Zabrocki, J., et al., J. Org. Chem., 57(1) (1992) 202–209.
48. Muller, G., et al., Proteins: Structure, Function, and Genetics, 15 (1993) 235–251.
49. Kahn, M., et al., J. Med. Chem., 34(12) (1991) 3395–3399.
50. Nakanishi, H., et al., Proc. Natl. Acad. Sci. USA, 89(March) (1992) 1705–1709.
51. Chen, S., et al., Proc. Natl. Acad. Sci. USA, 89 (1992) 5872–5876.
52. Gardner, B., H. Nakanishi, and M. Kahn, Tetrahedron, 49(17) (1993) 3433–3448.
53. Arrhenius, T. and A.C. Satterthwait, in *Peptides: Chemistry, Structure and Biology*, J.E. Rivier and G.R. Marshall, Editors. ESCOM Scientific Publishers, Leiden, (1990) 870–872.
54. Callahan, J.F., et al., Tetrahedron Lett., 49(17) (1993) 3479–3488.
55. Hermkens, P.H.H., et al., Tetrahedron Lett., 35(49) (1994) 9271–9274.
56. Virgilio, A.A. and J.A. Ellman, J. Am. Chem. Soc., 116 (1994) 11580–11581.
57. Ku, T.W., et al., J. Am. Chem. Soc., 115 (1993) 8861–8862.
58. Ripka, W.C., et al., Tetrahedron, 49(17) (1993) 3609–3628.
59. Ripka, W.C., et al., Tetrahedron, 49(17) (1993) 3593–3608.
60. Marshall, G.R., et al., in *Peptide Chemistry 1992, Proc. 2nd Japanese Symposium on Peptide Chemistry*, N. Yanihara, Editor. ESCOM Scientific Publishers, Leiden, (1993) 474–478.
61. Olma, A., et al. in *Peptides: Chemistry, Structure and Biology (13th American Peptide Symposium)*. ESCOM Scientific Publishers, Leiden (1994).
62. Kolodziej, S.A., et al., J. Med. Chem., 38(1) (1995) 137–149.
63. Kolodziej, S.A. and G.R. Marshall, Int. J. Pept. Protein Res., 48 (1996) 274–280.
64. Makara, G.M. and G.R. Marshall, Tetrahedron Letters, 38(29) (1997) 5069–5072.
65. Aston, K.W., et al., Tetrahedron Lett., 35(22) (1994) 3687–3690.
66. Riley, D.P., et al., J. Am. Chem. Soc., 119(28) (1997) 6522–6528.
67. Zhang, D., et al., Inorg. Chem., 37(5) (1998) 956–963.
68. Franklin, G.W., D.P. Riley, and W.L. Neumann, Coordination Chemistry Reviews, 174 (1998) 133–146.
69. Riley, D.P., et al., Inorg. Chem., 38 (1999) 1908–1917.
70. Riley, D.P., Chem. Rev., 99(9) (1999) 2573–2587.
71. Riley, D.P., Adv. Supramolecular Chem., 6 (2000) 217–244.
72. Aston, K.W., et al., Inorg. Chem., 40 (2001) 1779–1789.
73. SYBYL6.8^{TM}, *Molecular Modeling System*, Tripos Associates, Inc., St. Louis, Mo.
74. Riley, D.P., et al., Inorg. Chem., 35(18) (1996) 5213–5231.
75. Carlsson, A.E., Phys. Rev. Lett., 81(2) (1998) 477–480.
76. Carlsson, A.E. and S. Zapata, Biophysical J., 81 (2001) 1–10.
77. Ho, C.M.W. and G.R. Marshall, J. Comput. Aided Mol. Des., 7 (1993) 3–22.
78. Weiner, S.J., et al., J. Comp. Chem., 7(2) (1986) 230.
79. Mao, B., Biochem. J., 288 (1992) 109–116.
80. Lauri, G. and P.A. Bartlett, J. Comput. Aided Mol. Des., 8(1) (1994) 51–66.
81. Martin, Y., et al., J. Comput. Aided Mol. Des., 2(1) (1988) 15–29.
82. Granger, P., *Transition Metal Nuclear Magnetic Resonance, Studies in Inorganic Chemistry*, P.S. Regosin, Editor. Elsevier, Amsterdam (1991) 264–346.
83. Huheey, J.E., *Inorganic Chemistry: Principles of Structure and Reactivity*. Harper and Row, New York (1983).